Effects of self-assembled gold nanoparticles on $YBa_2Cu_3O_{7-\delta}$ thin films and devices

P. Michalowski[1], **C. Katzer**[1], **F. Schmidl**[1] **and P. Seidel**[1]

[1] Institut für Festkörperphysik, Friedrich-Schiller-Universität Jena, D-07743 Jena, Germany

Peter.Michalowski@uni-jena.de

Abstract. In our work we prepared $YBa_2Cu_3O_{7-\delta}$ (YBCO) thin films with self-assembled gold nanoparticles on $SrTiO_3$ (STO) substrates. We carried out different experiments to determine the effects on the crystallographic properties of the YBCO matrix as well as of the gold nanoparticles. Furthermore, we investigated how the particles influence the superconducting parameters of the film, e.g. the critical temperature T_C and the critical current density j_C. To ascertain j_C we employed magneto-optical Faraday microscopy. In addition, the YBCO film was deposited and structured on STO bi-crystal substrates, thus producing grain boundary Josephson junctions. We studied those junctions with respect to the normal state resistance R_N, and the dependence of the critical current I_C on the temperature T as well as on the magnetic flux Φ. Finally, we prepared direct current superconducting quantum interference device (dc-SQUID) gradiometers and embedded gold nanoparticles at well-defined areas such as only the antenna or the SQUID region. We measured the flux noise in a shielded environment using an ac-bias reversal technique and compared it with that of sensors without gold nanoparticles. Thus, we demonstrate a new preparation method and an innovative application of gold nanoparticles.

1. Introduction

YBCO is one of the best known high temperature superconductors and is used for superconducting thin film devices for more than twenty years. There are different approaches to the realization of dc-SQUIDs and dc-SQUID gradiometers [1, 2]. Noise characteristics have been studied thoroughly and have shown that a small critical current I_C is favorable to minimize the contribution of current noise [3]. On the other hand, especially for applications in planar gradiometer structures, a high critical current density in the antenna areas crossing the grain boundary is necessary [4]. Therefore an independent optimization of the critical current density of YBCO thin films across the grain boundary in the region of the Josephson junctions and in the region of the antennas is very helpful. The scaling law between the critical current density of the Josephson junction j^{JJ}_C and I_CR_N is $I_CR_N \sim (j^{JJ}_C)^n$ with $n \approx 0.5$ [5]. In former investigations on grain boundary engineering a reduction of I_C correlated with a decrease of the I_CR_N product [6]. This is unfavorable, because a high I_CR_N product enables high transfer functions for SQUID applications [7]. In our current work we are following another approach: adjusting the properties of bi-crystal grain boundary Josephson junctions by using gold nanocrystals [8].

During the last years there have been various attempts to manipulate the properties of superconducting thin films by using nanoparticles. We are going to give a short summary of different approaches by other groups.

The superconducting properties of the YBCO films like critical temperature T_C, critical current density j_C and critical magnetic fields H_{C1} and H_{C2} of the type II superconductor depend on the oxygen stoichiometry as well as on the crystal structure and the possible structure of defects. Therefore, it is possible to influence a lot of experimental parameters through the embedding of nanoparticles in the YBCO matrix. There is the chance to reduce the interface resistance [9]. Artificial pinning centers (APCs) can be created by adding non-superconducting material to the target [10], when depositing the film by pulsed laser deposition (PLD). Another approach to generate APCs is the preparation of the substrate with arrays of non-superconducting particles before the deposition of the superconducting film [11]. Mikheenko et al. report an improvement of flux pinning leading to an increase of j_C [12, 13]. The difference to our work is that the particles have either been on the surface of the film [11] or at the interface to the substrate [14]. This leads to 1D or 2D APCs with a strong angular dependence of the $j_C(B)$ characteristics, where B is the magnetic induction [15]. A combination of different APCs and the arising improvement of j_C are presented by Ercolano et al. [16].

In contrast to the widely-used method to embed nanoparticles in thin films we do not use non-superconducting additives to the target. We prepared very thin gold films which cluster during the deposition of the subsequent film of YBCO leading to self-organized crystalline nanoparticles Besides, the technique developed by us enables the systematic modification and optimization of selected regions of the sample.

2. Sample Preparation

We prepared our samples on polished STO (001) single-crystal substrates with sizes of 5 x 10 mm² and 10 x 10 mm². Using PLD we started with an initial gold layer with a thickness of 1 to 5 nm. This process was executed with a KrF excimer laser (λ = 248 nm, τ = 25 ns) at a repetition rate of 10 Hz and a laser fluence of 1.3 J/cm² under high vacuum conditions ($p_0 < 5 \cdot 10^{-4}$ Pa). With these parameters we achieved homogeneous Au-growth at a rate of approximately 4 nm/min. To get comparable YBCO films with and without gold nanocrystals on one substrate we used a shadow mask to cover one half of the substrate. After the deposition of the gold layer the shadow mask was removed and the substrate was heated to 780°C leading to a clustering of the gold. Using the KrF excimer laser again, a 150 nm thick YBCO layer was deposited in an oxygen atmosphere of p_{O2} = 50 Pa. To achieve optimum growth conditions, the repetition rate was set to 5 Hz and the laser fluence to 2.2 J/cm2. Under these conditions the growth rate was 20 nm/min. After deposition the substrate was cooled down to room temperature at a rate of 50 K/min in an atmosphere of pure oxygen ($p_{O2} = 8 \cdot 10^4$ Pa). During this process, gold nanoparticles evolved from the initial layer (see figure 1). If electrical characterization was planned, a 20 nm thick gold layer was deposited by dc-sputtering using a shadow mask to provide a bonding area. Finally, a possible structuring of the sample was performed using photolithography and ion beam etching. For the latter we attached the samples to a liquid-nitrogen-cooled sample holder. Applying an acceleration voltage of 500 V and an ion current density of 1 mA/cm² an etching rate of 20 to 30 nm/min, depending on the angle between ion beam and sample, was achieved. In this process, the superconducting properties of the YBCO films were not affected.

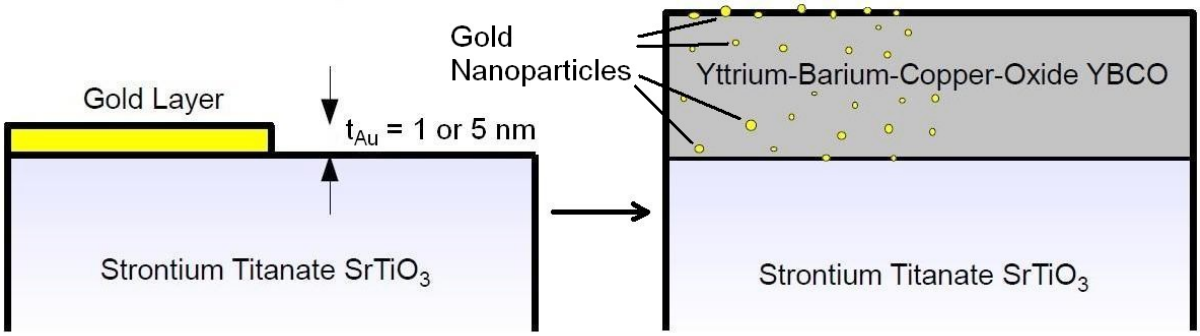

Figure 1. Scheme of the formation of the gold nanoparticles.

For the preparation of Josephson junctions, dc-SQUIDs or dc-SQUID gradiometers we used 10 x 10 mm² STO bi-crystal substrates with grain boundary angles of 24° as well as of 36.8° and carried out the steps mentioned above. In addition to the application of a shadow mask we went for another approach to produce regions with and without gold nanocrystals: To restrict the nanocrystals only to well defined positions, e.g. only the SQUID or only the antenna structures, we used spin coating to apply the photoresist AZ5214E from Microchemicals to the cleaned substrates. After the exposure of our samples to ultraviolet light and development of the structure we went on with the deposition of the gold layer and subsequently stripped off the remaining photoresist.

3. YBCO films with gold nanoparticles

TEM images show a distribution of the gold nanoparticles in the entire YBCO film, e.g. they can be found at the interface to the STO substrate, in the film and at the surface [17, 18]. The particles are found to be crystalline and orientated in (111) or (110) direction with regard to the substrate normal. Also in the case of changes in the preparation conditions, e.g. substrate temperature, we found that the gold nanocrystals influence the growth of the YBCO film. SEM images show a reduced roughness by less voids and no spiral growth as well as fewer outgrowths in the vicinity of the gold nanocrystals (figure 2) [17]. Furthermore, a-axis growth (needle-like structures seen in the left side of figure 2) can be completely prevented in the modified regions. Enhanced pinning of flux vortices leads to a significant increase of the critical current density j_C, which is shown on patterned samples via transport measurements as well as for unpatterned regions via magneto-optical Faraday microscopy [18]. Another positive effect of the gold nanoparticles is the slightly increased critical temperature T_C.

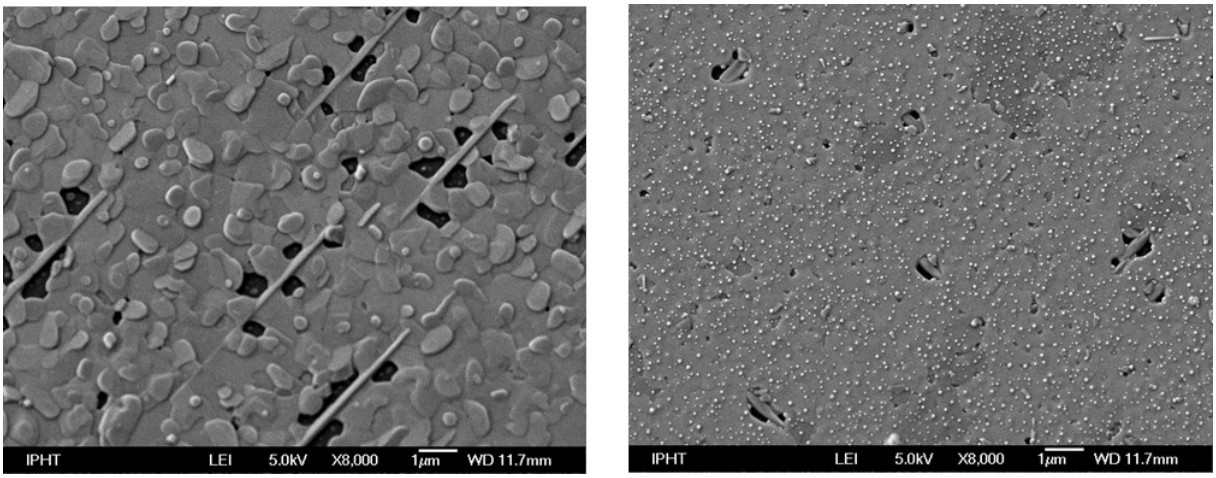

Figure 2. SEM images of a YBCO film with (left) and without (right) gold nanoparticles.

4. Grain boundary Josephson junctions, dc-SQUIDs and dc-SQUID gradiometers

In addition to YBCO films we also prepared bi-crystal grain boundary Josephson junctions and characterized them. We found, that the gold nanoparticles cause a modification of the superconducting parameters of the YBCO film crossing the grain boundary. Measuring the dependence of the critical Josephson current I_C on the magnetic induction B, I_C was more suppressed for Josephson junctions with gold nanocrystals [8]. Thus, we assume a smaller amount of a possible leakage current compared to junctions without gold nanoparticles. Unlike for YBCO films without grain boundary I_C is reduced for gold-modified junctions. We measured the temperature dependence of I_C for the SQUIDs S2 (initial gold layer thickness of 3 nm) and S9 (5 nm). As figure 3 shows I_C of S9 is smaller than that of S2 over the whole temperature range.

Both curves exhibit the typical behavior of grain boundary Josephson junctions in high-T_C superconductors [19]. This indicates that the gold nanocrystals do not change the transport mechanism of Cooper pairs, whereas the value of the critical current is significantly different depending on the thickness of the initial gold layer. Since this decrease in I_C is correlated with an increase of the normal state resistance R_N the I_CR_N product stays nearly constant [8]. Figure 4 illustrates this fact by showing data of Josephson junctions on two different samples, each containing junctions with and without gold nanoparticles. While I_C is reduced by a factor of 1.5 to 2 the I_CR_N product does not change. As the transfer function of a dc-SQUID depends on the I_CR_N product, the decrease of the critical current without a reduction of the I_CR_N product should be in favor of a high transfer function. This opens up new interesting perspectives for the improvement of sensors based on bi-crystal grain boundary Josephson junctions.

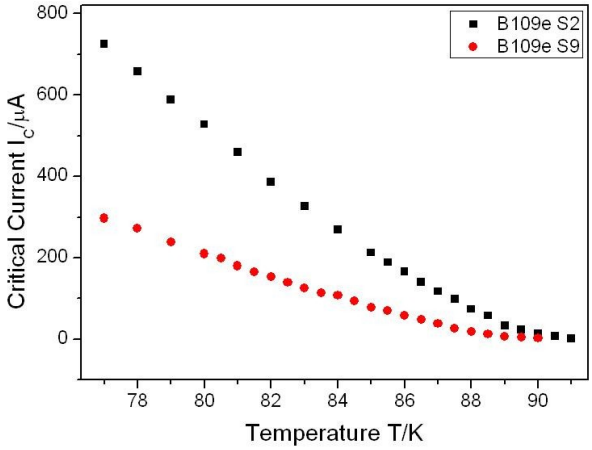

Figure 3. Critical current I_C of SQUIDs B109e S2 (3 nm initial gold layer) and S9 (5 nm initial gold layer) depending on temperature T.

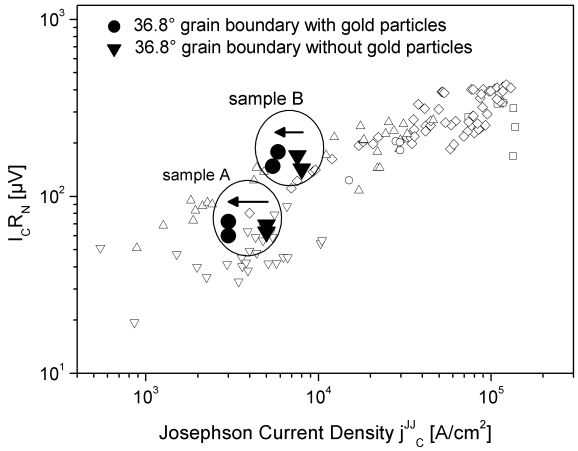

Figure 4. I_CR_N (j^{JJ}_C) characteristics of bi-crystal grain boundary Josephson junctions with and without gold nanoparticles. The open symbols denote data from past measurements and illustrate the general dependence of the two parameters.

To study the modulation depth ΔV or transfer function we also exposed the SQUIDs to the varying magnetic field of a small coil and measured the dependence of the voltage V on the coil current I_{coil} for different bias currents I_B. We found modulations for SQUIDs with different initial gold thicknesses. An example can be seen in figure 5.

The influence of LC-resonances in the I-V-curves of the dc-SQUID is clearly visible as different maxima and minima occur. To compare ΔV of different SQUIDs we carried out modulation measurements for different temperatures and ascertained ΔV for the respective I_B. Data for SQUID B109e S9 is given in figure 6 and shows a higher maximum ΔV for the SQUID with the larger initial

gold layer. For all investigated SQUIDs ΔV passes through several maxima and rises with smaller temperatures T. An interesting point is the shift of the maximum of ΔV from the first peak at lower I_B to the second peak with lower temperatures, a behavior we observed for the first time. In contrast to former investigations of dc-SQUID structures with the same geometry and film thickness we found that from around 70 K downwards the second maximum starts to dominate the transfer function.

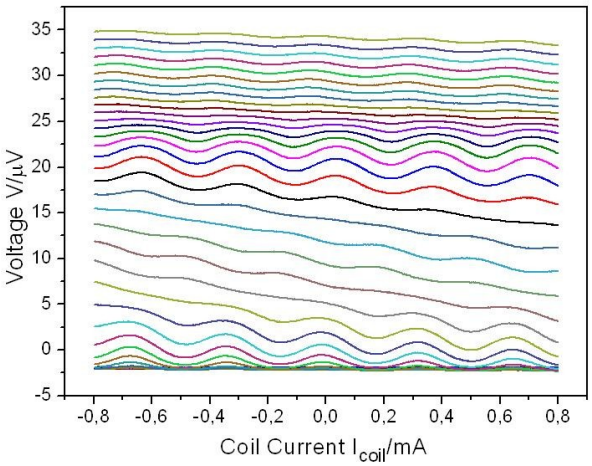

Figure 5. Modulation curves of SQUID B109e S9 for bias currents I_B=190..780 μA at T=69 K.

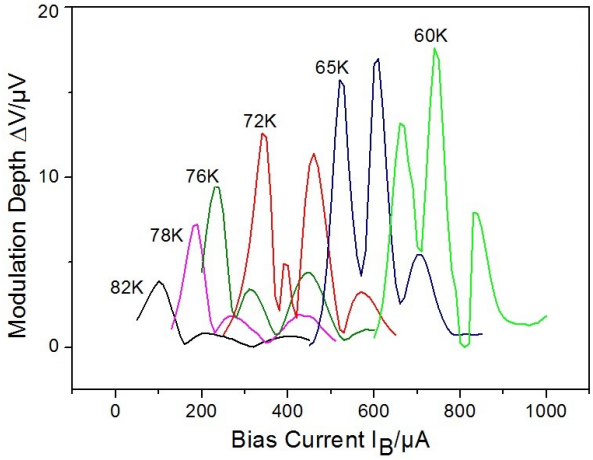

Figure 6. Modulation depth ΔV depending on bias current I_B of B109e S9 measured for different temperatures.

As stated above, additional pinning centers should not only increase the critical current density of the YBCO thin film, but also influence the noise properties of the dc-SQUID gradiometer. First noise measurements indicate improved voltage or flux noise characteristics [18]: We achieved a white noise between 5 $\mu\Phi_0/\sqrt{Hz}$ and 6 $\mu\Phi_0/\sqrt{Hz}$ with our gold-modified gradiometers. This is a very low value compared to conventional SQUID gradiometers based on bi-crystal Josephson junctions, as it is comparable to the best values reported for single dc-SQUIDs without antenna structures. Furthermore, we did also observe a shift of the corner frequency of the 1/f noise from about 10 Hz (as reported for gradiometers used in biomagnetic systems [20]) to a frequency of about 2 Hz. This is a far more interesting point because it strongly influences the sensor performance in the low frequency range e.g. at 1 Hz. Nevertheless, the impact of the thickness of the initial gold layer on the noise properties has not been investigated yet.

5. Summary

In conclusion, we have developed a new application of gold nanoparticles. Self-assembling from an initial gold layer during the growth of the YBCO film, these crystalline particles modify the superconducting properties of the latter in a favorable way. Used in plain YBCO films the nanoparticles lead to an enhancement of the critical current density j_C. At Josephson junctions they decrease the critical Josephson current I_C while increasing the normal state resistance R_N leading to an unchanged I_CR_N product. Using photolithography the nanoparticles can be restricted to certain regions of the sample. Therefore, an adjustment of e.g. the critical current density j_C in determined areas on a single substrate can be achieved. This opens up the possibility to tune the parameters of superconducting devices based on grain boundary Josephson junctions.

Furthermore, it is also possible to expand this technique to other films than YBCO, e.g. STO. In this case a modification of the optical properties could be observed [21].

Acknowledgement
The authors would like to thank J. Albrecht, S. Treiber, C. Stahl, V. Grosse, D. Kuhwald, M Schmidt, U. Hübner and S. Koch for their support. C. Katzer would like to thank the Landesgraduiertenförderung Thüringen for financial support.

References

[1] Peiselt K, Schmidl F, Linzen S, Anton A S, Hübner U and Seidel P 2003 *Supercond. Sci. Tech.* **16** 1408–12
[2] Zakosarenko V, Schmidl F, Schneidewind H, Dörrer L and Seidel P 1994 *Appl. Phys. Lett.* **65**, 779
[3] Il'ichev E, Dörrer L, Schmidl F, Zakosarenko V, Seidel P and Hildebrandt G 1996 *Appl. Phys. Lett.* **68** 708
[4] Steppke A, Becker C, Grosse V, Dörrer L, Schmidl F, Seidel P, Djupmyr M and Albrecht J 2008 *Appl. Phys. Lett.* **92** 122504
[5] Gross R, Chaudhari P, Kawasaki M and Gupta A 1990 *Phys. Rev B, Condensed matter* **42** 10735–37
[6] Wunderlich S, Schmidl F, Dörrer L, Schneidewind H and Seidel P 1999 *IEEE T. Appl. Supercon.* **9** 71
[7] Enpuku K, Shimomura Y and Kisu T 1993 *J. Appl. Phys.* **73** 7929–34
[8] Michalowski P, Schmidt M, Schmidl F, Grosse V, Kuhwald, D, Katzer C, Hübner U and Seidel P 2011 *Phys. Status Solidi RRL* **5** 268.
[9] Caton R, Selim R, Buoncristiani A M and Byvik C E 1990 *J. Appl. Phys.* **67** 7478–82
[10] Pinto R, Apte P R, Rao M S R, Chandra R, D'Souza C P, Pai S P, Gupta L C,Vijayaraghavan R, Gnanasekar K I and Sharon M 1996 *Appl. Phys. Lett.* **68** 1006–8
[11] Lengl G, Ziemann P, Banhart F and Walther P 2003 *Physica C: Superconductivity* **390** 175–84
[12] Mikheenko P, Abell J S, Sarkar A *et al.* 2010 . *J. Phys.: Conference Series* **234** 022022
[13] Mikheenko P, Dang V-S, Kechik M M A, Sarkar A, Paturi P, Huhtinen H, Abell J S and Crisan A 2011 *IEEE T. Appl. Supercon.* **21** 3184–8
[14] Mikheenko P, Tanner J L, Bowen J, Sarkar A, Dang V-S, Abell J S and Crisan A 2010 *Physica C: Superconductivity* **470** 234–6
[15] Matsumoto K and Mele P 2010 *Supercond. Sci. Tech.* **23** 014001
[16] Ercolano G, Bianchetti M, Wimbush S C, Harrington S A, Wang H, Lee J H and MacManus-Driscoll J L 2011 *Supercond. Sci. Tech.* **24** 095012
[17] Grosse V, Engmann, Schmidl F, Undisz A, Rettenmayr M and Seidel P 2010 *Phys. Status Solidi RRL* **4** 97–9
[18] Katzer C, Schmidt M, Michalowski *et al.* 2011. *Europhys. Lett.* **95** 68005
[19] Hilgenkamp H, Mannhart J 2002 *Rev. Mod. Phys.* **74** 485–549
[20] Weidl R, Brabetz S, Klemm F, Dörrer L, Schmidl F and Seidel P 1997 *Cryogenics* **37** 691-3
[21] Christke S, Katzer C, Grosse V, Schmidl F, Schmidl G, Fritzsche W, Petschulat J, Pertsch T and Rettenmayr M 2011 *Optical Materials Express* **1** 890-7